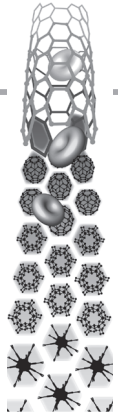

Citrullination of proteins: a common post-translational modification pathway induced by different nanoparticles *in vitro* and *in vivo*

Aim: Rapidly expanding manufacture and use of nanomaterials emphasize the requirements for thorough assessment of health outcomes associated with novel applications. Post-translational protein modifications catalyzed by Ca^{2+}-dependent peptidylargininedeiminases have been shown to trigger immune responses including autoantibody generation, a hallmark of immune complexes deposition in rheumatoid arthritis. Therefore, the aim of the study was to assess if nanoparticles are able to promote protein citrullination. **Materials & methods:** Human A549 and THP-1 cells were exposed to silicon dioxide, carbon black or single-walled carbon nanotubes. C57BL/6 mice were exposed to respirable single-walled carbon nanotubes. Protein citrullination, peptidylargininedeiminases activity and target proteins were evaluated. **Results:** The studied nanoparticles induced protein citrullination both in cultured human cells and mouse lung tissues. Citrullination occurred via the peptidylargininedeiminase-dependent mechanism. Cytokeratines 7, 8, 18 and plectins were identified as intracellular citrullination targets. **Conclusion:** Nanoparticle exposure facilitated post-translational citrullination of proteins.

Original submitted 18 March 2011; Revised submitted 10 November 2011; Published online 25 May 2012

KEYWORDS: autoimmunity ■ high content analysis ■ immune system ■ inflammation ■ nanomaterial ■ nanoparticle ■ peptidylargininedeiminase ■ post-translational modification ■ protein citrullination ■ rheumatoid arthritis

Bashir M Mohamed‡, Navin K Verma‡, Anthony M Davies, Aoife McGowan, Kieran Crosbie-Staunton, Adriele Prina-Mello, Dermot Kelleher, Catherine H Botting, Corey P Causey, Paul R Thompson, Ger JM Pruijn, Elena R Kisin, Alexey V Tkach, Anna A Shvedova* & Yuri Volkov*

**Authors for correspondence:*
Department of Clinical Medicine, Trinity College Dublin, Ireland
yvolkov@tcd.ie
and
Health Effects Laboratory Division, NIOSH, Morgantown, WV, USA
ats1@cdc.gov
‡Authors contibuted equally
For a full list of affiliations please see page 1195

Recent progress in nanotechnology has enabled the manufacturing of nanosized materials for various applications ranging from information technologies to advanced composite materials, consumer products, healthcare and life sciences. Because of their fascinating physicochemical properties, nanomaterials exhibit unique bioactivity. However, there remains considerable uncertainty regarding the potential risk to human health related to the widespread production and use of nanomaterials. Numerous epidemiological studies have associated exposure to ambient ultra-fine carbonaceous particles in air pollution to various diseases, including chronic obstructive pulmonary disease, pneumonia, heart attacks, autoimmune disorders and all-cause mortality increased with longer time scales [1–9]. It has been reported earlier that silica exposure is associated with increased risk of developing rheumatoid arthritis (RA) [10]. Moreover, smoking, which has long since been considered a nonspecific risk factor causing chronic inflammation, is now known to be associated with autoimmune diseases such as RA [9,11,12].

Chronic inflammatory diseases affect millions of people across the globe leading to untold suffering, economic burden and premature death. Recent studies have identified inflammation and the recruitment of immune cells to the site injury with a unique role for IL-1β activating platforms, known as inflammasomes, in the regulation/induction and pathogenesis of multiple autoimmune and inflammatory disorders [13]. Inflammation caused by airborne particles is associated with respiratory ailments including chronic obstructive pulmonary disease and autoimmune diseases, for example, RA [1,8,9,14]. It has been well documented that nanoparticles (NPs) are efficiently internalized by epithelial cells and professional phagocytes. Size- and dose-dependent cellular uptake, toxicity, stimulation/release of proinflammatory mediators and formation of nucleoplastic protein aggregates were reported in BEAS2, THP-1, and A549 cells treated with nanosized amorphous silica [15–18]. Single-walled carbon nanotubes (SWCNTs) functionalized by phosphatidylserine, were efficiently internalized by different phagocytic cells, such as murine RAW264.7 macrophages, primary monocyte-derived human macrophages, dendritic cells and rat brain microglia, for example [19]. It was also documented that SWCNTs localized in lysosomal compartments of alveolar macrophages after pulmonary exposure [19]. Oxidative stress

Future Medicine part of fsg

induced by micro-/nano-sized particles has been reported to cause protein modifications leading to compromised protein recognition, perhaps contributing to autoimmunity [20].

Antibodies to citrullinated proteins have a high diagnostic value in RA and are linked to the pathogenesis of several autoimmune diseases [12,21–25]. Citrullinated proteins are generated by a post-translational deimination of polypeptide-bound arginine by a family of Ca^{2+}-dependent enzyme peptidylarginine deiminase (PAD) [22,26,27]. Several isotypes of PAD exist, each with different tissue distribution [26–28]. PAD2 and PAD4 are most important as they are widely expressed in a variety of tissues, including hematopoietic cells [26–28]. Citrullination results in a loss of net positive charge of molecules and causes significant biochemical changes and/or protein conformational changes [22]. Citrullinated proteins/peptides are recognized as nonself proteins, and subsequently induce an autoimmune response [21,22,24,25,29]. Citrullination is essential for the formation of neutrophil extracellular traps [30]. Site-specific citrullination was reported to alter chemokine function [31–33]. We hypothesize that exposure of amorphous silicon dioxide (SiO_2), ultra-fine carbon black (ufCB) and SWCNTs to A549 epithelial and professional phagocyte THP-1 cells cause enhanced PAD activity via the increase of extracellular Ca^{2+}, thus facilitating protein citrullination. Here, we demonstrate that nanomaterials of distinct origin, morphology and physicochemical properties are able to induce protein citrullination via increased Ca^{2+}-mediated PAD activity in human cells and animals.

Materials & methods

Nanomaterials

The SiO_2 NPs; 30, 80 and 400 nm (Glantero Ltd, Cork, Ireland), positively-charged alumina-coated chloride ion-stabilized SiO_2 NPs (40 nm; LUDOX CL 420891, Sigma-Aldrich, MO, USA), sodium counterion stabilized SiO_2 NPs (20 nm; LUDOX CL 420883, Sigma-Aldrich, ufCB [Printex 90, Degussa, Germany]), and SWCNTs (Carbon Nanotechnologies Inc., TX, USA) were used. The physicochemical properties of SiO_2 NPs have previously been described [34]. The SWCNTs were manufactured using the high-pressure carbon monoxide disproportionation process. Purity assessment of high-pressure carbon monoxide disproportionation process SWCNTs was carried out by using several standard analytical techniques, including thermogravimetric analysis with differential scanning colorimetry, thermoprograming oxidation, and Raman and near infrared spectroscopy [35]. All the nanomaterials were dispersed in culture media. SWCNTs were sonicated (Branson Sonifier 450, CT, USA) before treatments.

Cell culture

Human lung epithelial cell line A549 and a phagocytic cell line THP-1 (ATCC, VA, USA) were cultured in DMEM and RPMI 1640 medium, respectively. Both the media were supplemented with 10% (v/v) fetal bovine serum, 1% (v/v) L-glutamine/penicillin/streptomycin. Cells were grown in a humidified incubator at 37°C in 5% CO_2. THP-1 cells were stimulated with phorbol 12-myristate 13-acetate (25 ng/ml) before experimentation.

Animals

Animal studies were carried out under the experimental protocol (#07-AS-M-010) approved by the Institutional Animal Care and Use Committee at the National Institute for Occupational Safety and Health (WV, USA). The National Institute for Occupational Safety and Health facilities are accredited by the Association for Assessment and Accreditation of Laboratory Animal Care–International Committee. Animals were supplied, housed and exposed as described previously [35]. Briefly, 20.0 ± 1.9 g C57BL/6 pathogen-free adult female mice (Jackson Laboratory, ME, USA) were housed in solitary cages supplied with high efficiency particulate-filtered air. Mice were given water and certified chow 7913 (Teklad, IN, USA) *ad libitum* in compliance with the policies of the Institute of Laboratory Animal Resources (National Research Council). Experimental and control groups were given equal volumes of SWCNTs (40 µg/mouse) or sterile magnesium- and calcium-free phosphate-buffered saline (PBS) solution by pharyngeal aspiration. Experimental and control groups were euthanized at 7 days, 28 days, 2 months and 6 months following exposures.

Antibodies & reagents

Rabbit polyclonal anticitrulline (cat# ab6464), rabbit monoclonal anticytokeratin 7, rabbit polyclonal anticytokeratin 8/18 and fluorescein isothiocyanate (FITC)-linked goat antirabbit antibodies were from Abcam (Abcam plc., Cambridge, UK). Immunoaffinity purified

rabbit polyclonal anticitrulline antibody used for western blot analysis was from Millipore (cat# 07-377, MA, USA). The specificity data of anticitrulline antibodies provided by the manufacturer showed high reactivity with citrulline, compared with very low cross-reactivity with homocitrulline (10^3-times higher for citrulline; Abcam plc., Cambridge, UK). Furthermore, in-house validation was assessed against the manufacturer's data (SUPPLEMENTARY FIGURE 1, see online at www.futuremedicine.com/doi/suppl/10.2217/nnm.11.177). Rabbit antihuman PAD2 and antihuman PAD4 antisera were produced by GJM Pruijn and WJ van Venrooij, Nijmegen, The Netherlands. Horseradish peroxidase-conjugated anti-rabbit IgG and antimouse IgG antibodies were from Dako A/S (Glostrup, Denmark). Cl-amidine was synthesized as described previously [36]. Unless attributed specifically, all the reagents were from Sigma-Aldrich, and plastic wares were from Nunc (Thermo Fisher Scientific Inc., MA, USA).

Analysis of protein citrullination

Cells were seeded in 96-well plates (1×10^4 cells/well), exposed to various concentrations of nanomaterials for multiple time points and fixed using 3% paraformaldehyde as described [37]. After gentle washing with PBS, cells were incubated with anticitrulline antibody (cat# ab6464, 1:200 dilution) for 1 h at room temperature. Cells were washed three times with PBS and then incubated with FITC-linked goat anti-rabbit antibody and Hoechst 33342 for 1 h. Plates were scanned using IN Cell Analyzer 1000 automated microscope (GE Healthcare, Buckinghamshire, UK). Images were acquired in a stereology configuration of five randomly selected fields per well at 20× magnification using two detection channels. These included a 4′,6-diamidino-2-phenylindole filter (channel 1: λ = 461 nm), which detected blue fluorescence indicating nuclear staining and FITC filter (channel 2: λ = 509 nm), which detected green fluorescence indicating citrullinated proteins. Protein citrullination was quantified using the dual area object analysis module of the IN Cell Investigator software (GE Healthcare, Buckinghamshire, UK). The module allows for simultaneous quantification of subcellular inclusions that are marked by different fluorescent labels and measures fluorescence intensity associated with predefined nuclear and cytoplasmic compartments.

Immunohistochemical staining & analysis

The lung tissue preparation including preservation and fixation was performed as previously described [35,38]. Immunohistochemical investigation for the presence of citrullinated proteins was conducted on 5-µm thick lung sections using the avidin–biotin–peroxidase complex detection procedure [39]. Stained tissue sections were digitally scanned using Aperio ImageScope™ and the images were analyzed automatically by ImageScope software (Aperio Technologies Inc., CA, USA), as described [40].

Cell lyses, immunoprecipitation, SDS-PAGE & western immunoblotting

The cell lysis, immunoprecipitation and western immunoblotting were performed as described previously [41,42].

Nano-liquid chromatography-electrospray ionization mass spectrometry/mass spectrometry

Bands of interest on colloidal coomassie blue-stained SDS-PAGE gel were excised and the proteins were identified by Nano-liquid chromatography-electrospray ionization mass spectrometry/mass spectrometry as described [43]. Ten or more matching peptides and a significant probability score ($p < 0.05$ = MOWSE score >150) were required for a secure identity assignment.

PAD enzyme activity measurements

Cells were exposed to the above indicated nanomaterials in triplicates for indicated time points and were lysed. PAD enzyme activity was determined by the ELISA method using ModiQuest Antibody Based Assay for PAD Activity (ABAP) kit according to the manufacturer's instructions (ModiQuest Research, Nijmegen, The Netherlands).

Measurements of intracellular Ca^{2+}

Cells were seeded in 96-well plate and allowed to adhere overnight. Following exposure to nanomaterials, cells were gently washed with prewarmed fresh medium. They were then incubated with 1 µM Hoechst 33342 and 1 µM Fluo-4 (fluo-4 acetoxymethyl ester) for 1 h. Plates were scanned using IN Cell Analyzer 1000 automated microscope (GE Healthcare). Images were acquired in a stereology configuration of five randomly selected fields per well at 10× magnification using two detection channels. Hoechst 33342 was visualized in the blue channel

(4′,6-diamidino-2-phenylindole filter) while Fluo-4 was visualized in the green channel (FITC filter). Intracellular free Ca^{2+} concentration was measured by the fluorescence intensity of Fluo-4 in a circular region (cellular compartment) centered at the nucleus and quantified using the dual area object analysis module of the IN Cell Investigator software (GE Healthcare).

Statistical analysis

Response of each cell type to various NPs was analyzed by two-way analysis of variance with

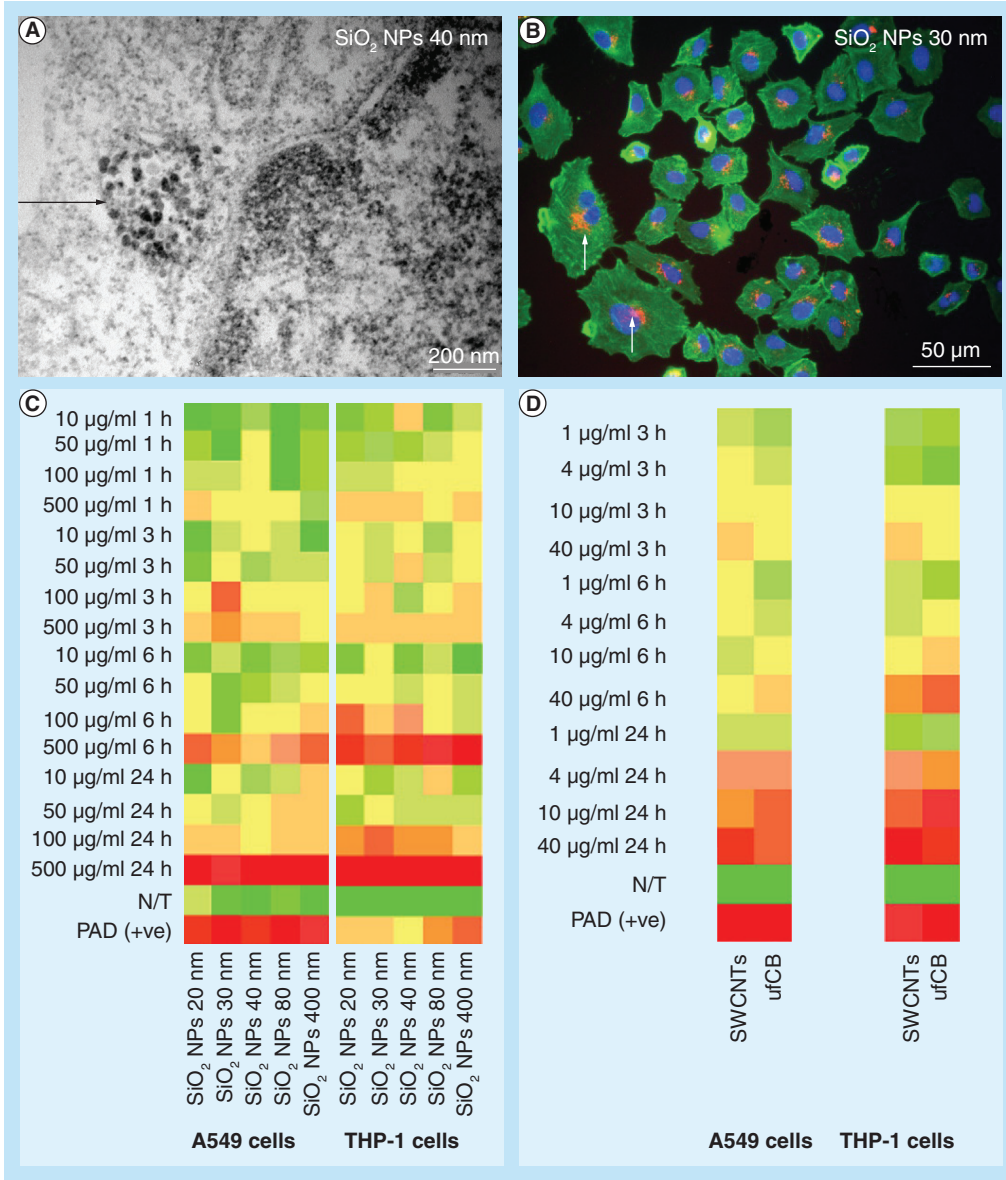

Figure 1. Cellular uptake of nanomaterials and induction of protein citrullination **(continued on page 1185).** **(A)** Transmission electron microscopy image of A549 cells exposed to 40 nm SiO_2 NPs for 3 h. The arrow indicates internalized SiO_2 NPs. **(B)** Fluorescent image of A549 cells exposed to tetramethyl rhodamine iso-thiocynate-labeled SiO_2 NPs (30 nm) for 3 h was acquired by an IN Cell Analyzer 1000 automated microscope using 20× objective. Arrows indicate internalized SiO_2 NPs. **(C & D)** A549 and THP-1 cells were exposed to indicated concentrations of SiO_2 NP (20, 30, 40, 80 or 400 nm), ufCB or SWCNT for 1–24 h. Cells were immunostained with anticitrulline antibody (cat# ab6464), imaged using automated microscope, and protein citrullination was quantified as presented in heatmaps. Heatmaps were generated for the above indicated protein citrullination and their colorimetric gradient table spans from: dark green: lower than 15% of maximum value measured; bright green: 30%; yellow: 50%; bright orange: 60%; dark orange: 75%; red: higher than 75% of the maximum value.
NP: Nanoparticle; N/T: No treatment; PAD: Peptidylargininedeiminase; SiO_2: Silicon dioxide; SWCNT: Single-walled carbon nanotube; ufCB: Ultra-fine carbon black.

Bonferroni post-test analysis. A p-value of <0.05 was considered to be statistically significant (GraphPad Prism 4, GraphPad Software, CA, USA). Konstanz Information Miner [101] data exploration platform and the screening module HiTS [102] were used to visualize the data [44–46]. The protein citrullination level induced by the nanomaterials was normalized using the percent of the positive controls. The Z score was used for scoring the normalized values. These scores were summarized using the mean function as follows: Z score = (x-mean)/standard deviation, as from previous work [47]. As previously described, Heatmap-type graphical illustration in a colorimetric gradient table format was adopted as the most suitable schematic representation to report on any statistical significance and variation from normalized controls based on their Z score values [46].

Results

Nanomaterials induced protein citrullination in human cells

Human lung epithelial A549 cells and phagocytic THP-1 cells were employed in this study. Transmission electron microscopy images showed internalization of SiO_2 NPs (40 nm) by A549 cells after exposure (3 h) (Figure 1A). Similar results were observed when A549 cells were exposed to fluorescently labeled SiO_2NP (30 nm) and examined by fluorescent microscopy (Figure 1B). To investigate the potential effect of nanomaterials on protein citrullination, A549 and THP-1 cells were exposed to various concentrations (10, 50, 100 or 500 µg/ml) of SiO_2 NPs (20, 30, 40, 80 or 400 nm), ufCB (1, 4, 10 or 40 µg/ml) or SWCNTs (1, 4, 10 or 40 µg/ml) for multiple time-points. High content analysis for the induction of protein citrullination was performed and heatmaps were generated (Figures 1C & 1D). The data indicated a significant increase in protein citrullination in both cell lines found in a time- and dose-dependent manner with maximum effects seen at 24 h (Figures 1C & 1D and Supplementary Figure 2–4). Immunofluorescent images of cells exposed to silica or carbon nanomaterials showed citrullinated proteins in the cytoplasm and around the nucleus (Figure 1E & Supplementary Figure 5).

To further validate if citrullinated proteins were expressed after 24 h in the cells treated with nanosized SiO_2 NPs, ufCB or SWCNTs, the cells were lysed and cell lysates were electrophoretically separated and probed with anticitrulline antibody (Millipore, cat# 07-377). Four distinct citrullinated protein bands were detected by this method (Figure 1F and Supplementary Figure 6), while a smear-like pattern appeared when the cell lysate was preincubated with PAD (Supplementary Figure 7). Densitometric quantitation of citrullinated protein bands were normalized by tubulin content indicating a significant fourfold increase in protein citrullination after NP exposures compared with those of respective unexposed controls (Figure 1F).

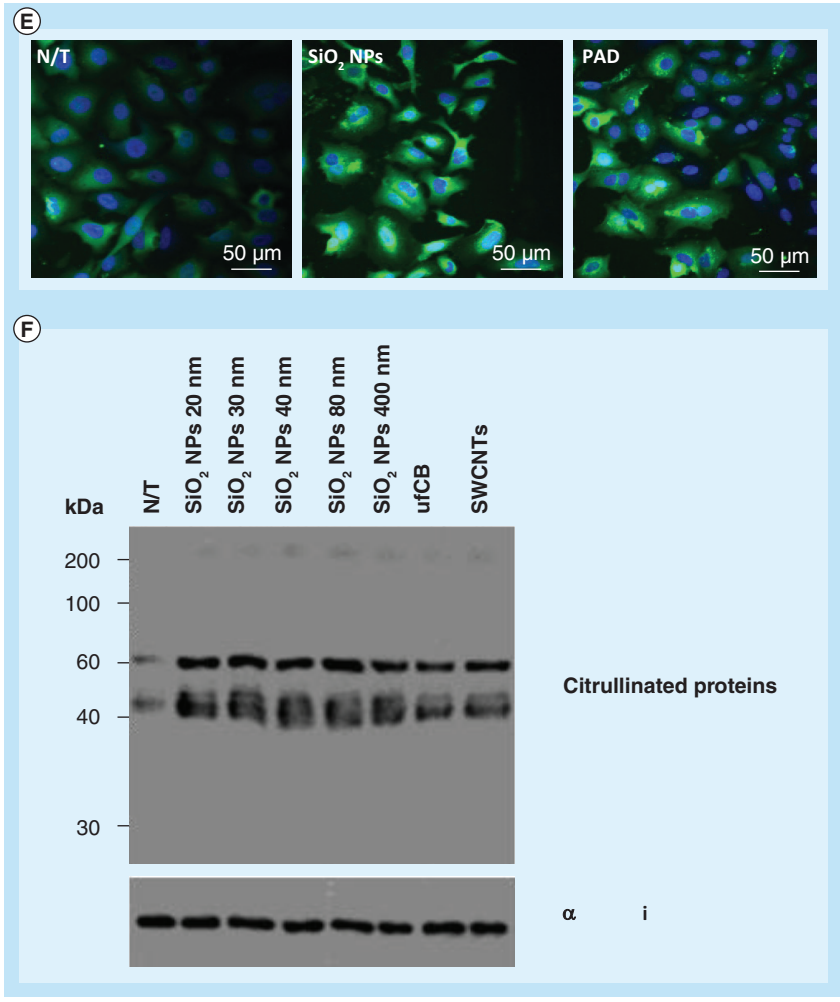

Figure 1 (continued from page 1184). Cellular uptake of nanomaterials and induction of protein citrullination. (E) A549 cells unexposed (N/T), exposed to 80 nm SiO_2 NPs or PAD (positive control) for 24 h and fixed in 3% paraformaldehyde. Cells were immunostained with anticitrulline antibody (cat# ab6464; green) and nuclei were stained with Hoechst (blue). Protein citrullination was visualized by IN Cell Analyzer 1000 using a 20× objective lens. **(F)** A549 cells (N/T) were exposed to 500 µg/ml SiO_2 NPs (20, 30, 40, 80 or 400 nm), 40 µg/ml ufCB or 40 µg/ml SWCNTs for 24 h and were then lysed. Cell lysates (50 µg each) were resolved by SDS-PAGE and after western blotting were probed for citrullinated proteins (Millipore, cat# 07-377) or tubulin. Results shown are representative of three independent experiments.
NP: Nanoparticle; N/T: No treatment; PAD: Peptidylargininedeiminase; SiO_2: Silicon dioxide; SWCNT: Single-walled carbon nanotube; ufCB: Ultra-fine carbon black.

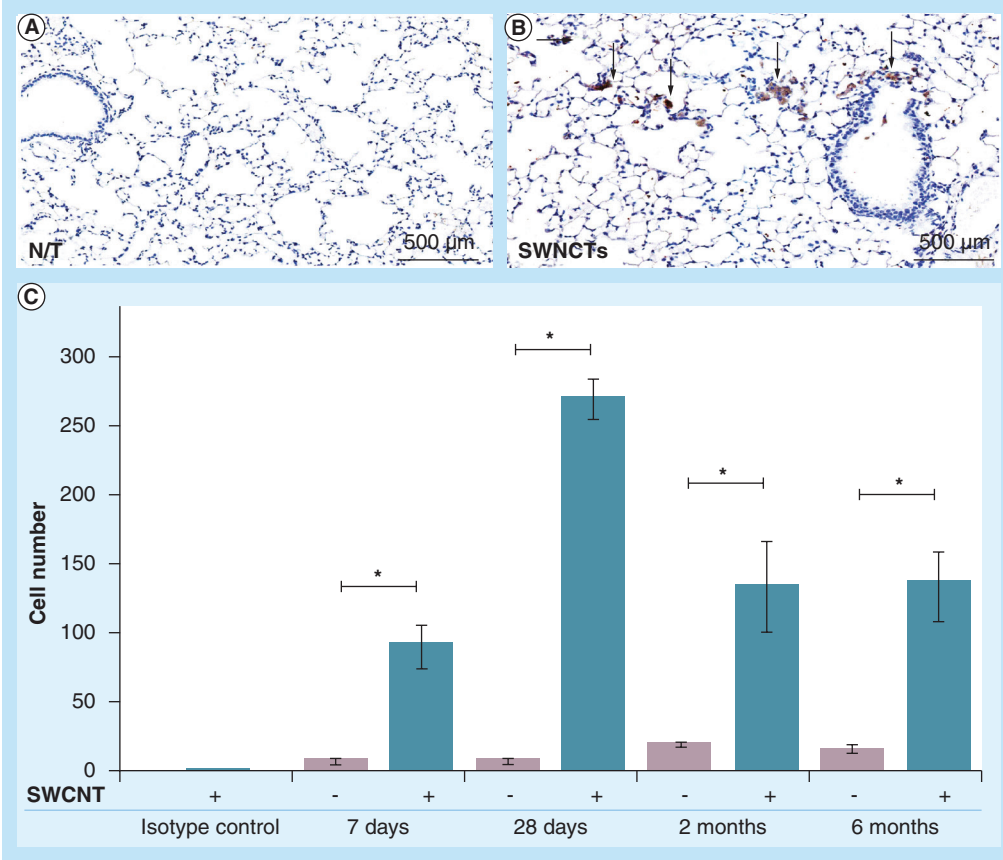

Figure 2. Immunohistochemical analysis of citrullinated proteins. Mice were exposed to SWCNT by pharyngeal aspiration and sacrificed on days 7, 28 and at 2 or 6 months. Lung tissue sections (5 µm thick) were prepared and stained immunohistochemically with anticitrulline antibody (cat# ab6464). **(A)** Lung tissue section from control mice. **(B)** Lung tissue section from SWCNT treated mice. Arrows indicate the anticitrulline antibody positive cells. **(C)** The induction of protein citrullination observed in the lung of mice following SWCNT exposure. The stained slides were digitally scanned and quantified as described in the 'Materials & methods' section. Statistical analysis was carried out by two-way analysis of variance with Bonferroni post-test analysis.
*Statistically significant data: $p < 0.001$.
N/T: No treatment; SWCNT: Single-walled carbon nanotube.

SWCNT exposure induced protein citrullination in mouse lung tissues

To investigate if exposure to respirable SWCNTs facilitated protein citrullination *in vivo*, C57BL/6 mice were given SWCNTs by pharyngeal aspiration. Lungs were harvested from mice during recovery time up to 6 months postexposure and the lung tissue sections were used for immunohistochemical staining against citrullinated proteins. Images were analyzed using Aperio ImageScope. Citrullinated proteins were not present in the lung tissue sections of control mice (Figure 2A), while images of lung tissues from SWCNT-exposed mice revealed immunoreactivity of citrullinated proteins (Figure 2B). Quantification of the immunostained tissues using ImageScope software indicated a significant increase in the number of cells bearing citrullinated proteins. The induction of protein citrullination was observed on day 7 following SWCNT exposure and the highest number of cells with citrullinated proteins was observed at day 28 (Figure 2C).

Exposure to nanomaterials activated PAD in human cells

Significantly higher PAD activity was observed in A549 and THP-1 cells exposed to SiO_2 NPs or ufCB (Figure 3). In particular, in A549 cells exposed to SWCNTs or SiO_2 NPs, activity of PAD was detectable after 3 h and peaked at 24 h (Figure 3A). In THP-1 cells exposed to SWCNTs or SiO_2 NPs significantly higher PAD activity was detected only at 24 h (Figure 3B). No changes in the expression levels of PAD isoforms, PAD2 and PAD4, after SiO_2 NP or SWCNT treatments were observed in A549

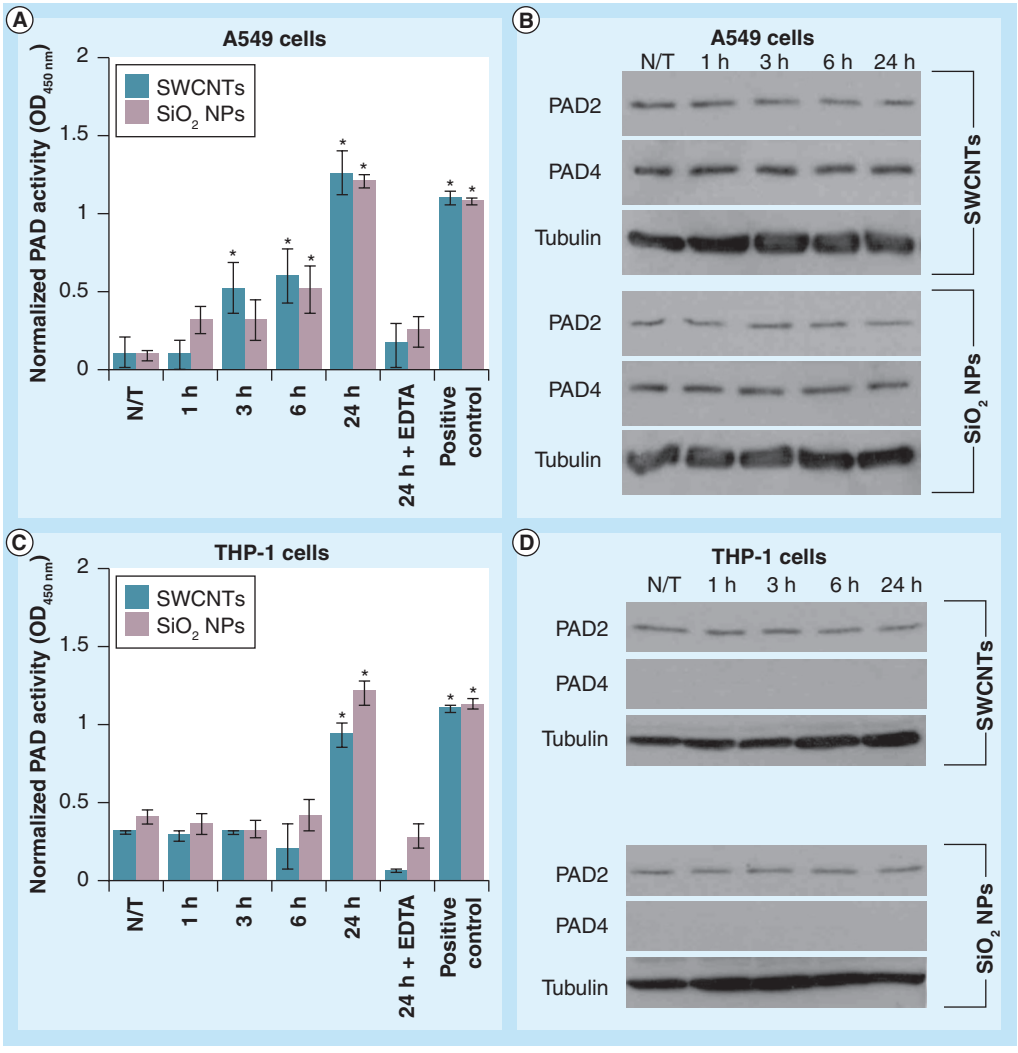

Figure 3. Peptidylargininedeiminase activity assays. (A & B) A549 and **(C & D)** THP-1 cells were exposed to 500 µg/ml 80 nm SiO_2 NPs or 40 µg/ml SWCNTs for 24 h and were then lysed. **(A & C)** The PAD enzyme activity in cell lysates (5 µg each) was determined and presented (mean $OD_{450\ nm}$ ± standard error of mean). **(B & D)** Cells were lysed, the lysates (50 µg each) were resolved by SDS-PAGE and after western blotting were probed for PAD2, PAD4 or tubulin. Results shown are representative of three independent experiments.
*Statistically significant data: $p < 0.05$.
NP: Nanoparticle; N/T: No treatment; OD: Optical density; PAD: Peptidylargininedeiminase; SiO_2: Silicon dioxide; SWCNT: Single-walled carbon nanotube.

cells assessed by western blotting (Figure 3C). In THP-1 cells, PAD2 expression was unchanged (Figure 3D).

Inhibition of PAD reduced protein citrullination in the cells treated with nanosized particles

To further validate the role of PAD activity in nanomaterial-induced protein citrullination in human cells, we used a synthetic inhibitor of PAD Cl-amidine. Cl-amidine is a well-characterized irreversible inhibitor of all PAD isozymes including PAD4 [48,49]. Cl-amidine was also shown to suppress PAD activity *in vivo* [30,50,51]. Pretreatment of A549 and THP-1 cells with various concentrations of Cl-amidine (50, 100 or 200 µM) resulted in a dose-dependent inhibition of SiO_2 NP- or SWCNT-induced PAD activity (Figures 4A & C). Since 100-µM concentration of Cl-amidine showed significant reduction in PAD activity with minimal effect on cell viability (Supplementary Figure 8), we selected this concentration for the following experimentation. Preincubation of A549 cells with C1-amidine resulted in significant reduction in SiO_2 NP- or SWCNT-induced protein citrullination (Figure 4B). However, preincubation of THP-1 cells with C1-amidine failed to abrogate NP-induced protein citrullination (Figure 4D).

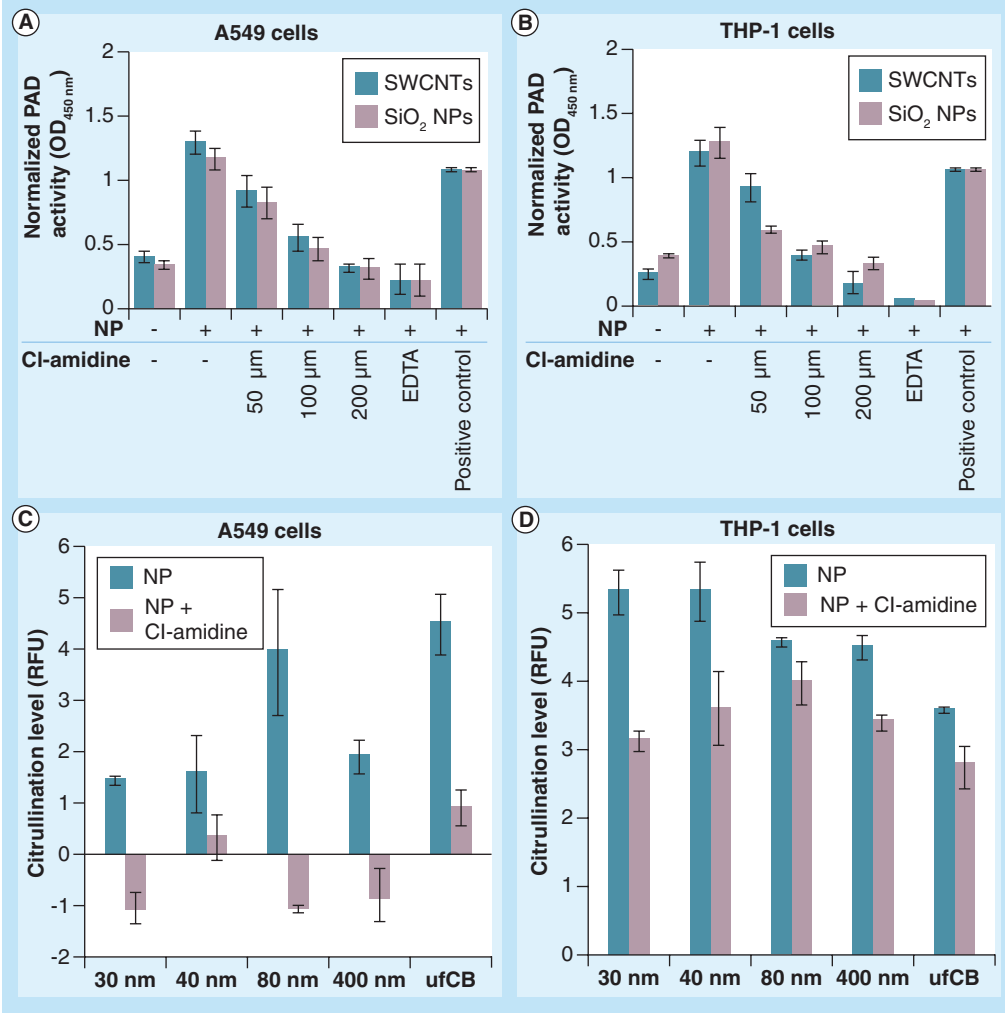

Figure 4. Effect of peptidylargininedeiminase inhibition on nanomaterial-induced protein citrullination. (A) A549 and **(B)** THP-1 cells were pretreated with 50, 100 or 200 µM Cl-amidine for 2 h and then exposed to SiO_2 NPs or SWCNTs for 24 h. The peptidylargininedeiminase enzyme activity in cell lysates (5 µg each) was determined by the ELISA method using ModiQuest antibody-based assay. Absorbance ($OD_{450\ nm}$) was measured and presented. Untreated or Cl-amidine pretreated **(C)** A549 or **(D)** THP-1 cells were exposed to various sizes of SiO_2 NPs or ultra-fine carbon black. Cells were immunostained with anticitrulline antibody (cat# ab6464) and imaged using automated microscope IN Cell Analyzer 1000 and quantified. Data are mean ± standard error of mean of three independent experiments performed in triplicates.
NP: Nanoparticle; OD: Optical density; PAD: Peptidylargininedeiminase; RFU: Relative fluorescence units; SiO_2: Silicon dioxide; SWCNT: Single-walled carbon nanotube; ufCB: Ultra-fine carbon black.

Ca^{2+} channel blocker inhibited nanomaterial-induced protein citrullination

Expression and the activation of PAD is required for protein citrullination. This activation requires local concentration of Ca^{2+} that are much higher than those in normal cytosolic conditions [52]. When THP-1 and A549 cells were exposed to SiO_2 NPs for 24 h, we observed an increased intracellular Ca^{2+} concentration compared with control cells (Figure 5). Employment of Ca^{2+} channel blocker (10 µM) and verapamil (Figure 5A) resulted in the inhibition of nanomaterial-induced protein citrullination observed in A549 cells (Figure 5C). In THP-1 cells inhibition of Ca^{2+} influx by verapamil (Figure 5B) did not fully block protein citrullination (Figure 5D).

Identification of proteins undergoing citrullination by proteomics

A549 cells exposed to SiO_2 NPs or ufCB for 24 h were lysed; cell lysates were immunoprecipitated by anticitrulline antibody (Millipore, cat# 07-377) and resolved by electrophoresis. Differentially citrullinated protein bands that were clearly present in SiO_2 NP- or ufCB-exposed cell lysates – four bands exhibiting

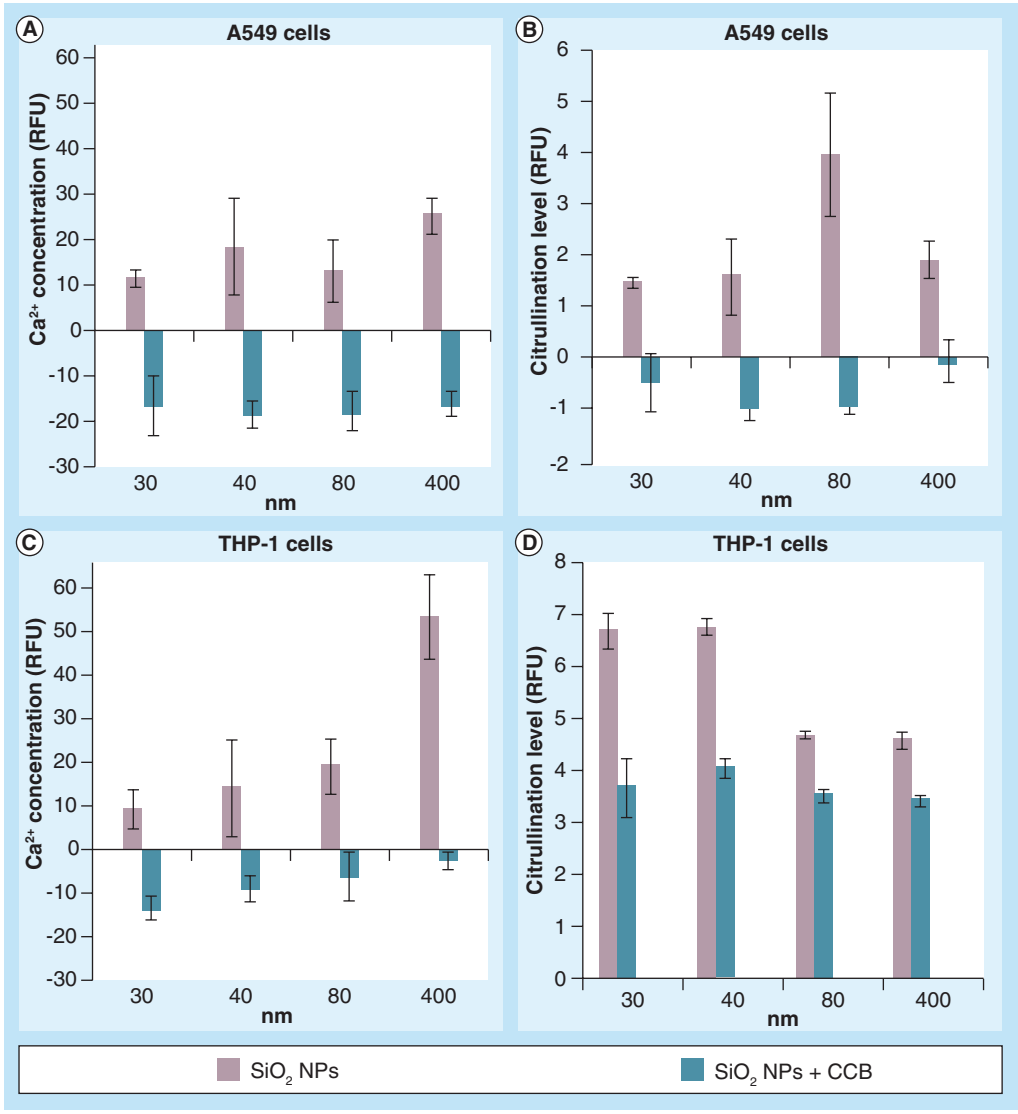

Figure 5. Intracellular Ca^{2+} levels in cells exposed to nanomaterials and the effect of blocking Ca^{2+} channels on protein citrullination. (A & B) A549 and **(C &D)** THP-1 cells were exposed to various sized SiO_2 NPs in the presence or absence of a Ca^{2+} CCB verapamil (10 μM). **(A & B)** Intracellular levels of free Ca^{2+} were measured and plotted as RFU. Verapamil treated or untreated cells were exposed to SiO_2 NP (30, 40, 80 or 400 nm) for 24 h, protein citrullination levels were analyzed and plotted as relative fluorescence units (RFU; **C & D**). Data are mean ± standard error of mean of three independent experiments performed in triplicates.
CCB: Ca^{2+} channel blocker; NP: Nanoparticle; RFU: Relative fluorescence units; SiO_2: Silicon dioxide.

strong intensity were excised from the gel (Figure 6A). These protein bands were subjected to mass spectrometry analysis as described under 'Materials & methods' section. Evaluation of the mass spectrometry/mass spectrometry data resulted in the identification of cytoskeletal proteins cytokeratin 7, 8, 18 and plectins (Figure 6A), and their citrullination sites (Supplementary Table 1). The presence of citrullination on cytokeratins was further validated biochemically. For this purpose, cell lysates from A549 control cells or those exposed to SiO_2NP (24 h) were separately immunoprecipitated with anticitrulline or anti-IgG (isotype control) antibodies and thereafter were assessed by western blotting using the specific antibodies against cytokeratin 7 (Figure 6B) or cytokeratin 8/18 (Figure 6C). As seen in Figure 6, the western blot analysis was consistent with the results obtained by mass spectrometry.

Discussion

Post-translational citrulination of proteins has been shown to alter their structure, antigenicity and functions. In RA, antibodies to cyclic citrullinated peptides are now well established for clinical diagnostics. The most commonly accepted molecular mechanism for autoimmunity associated with citrullinated

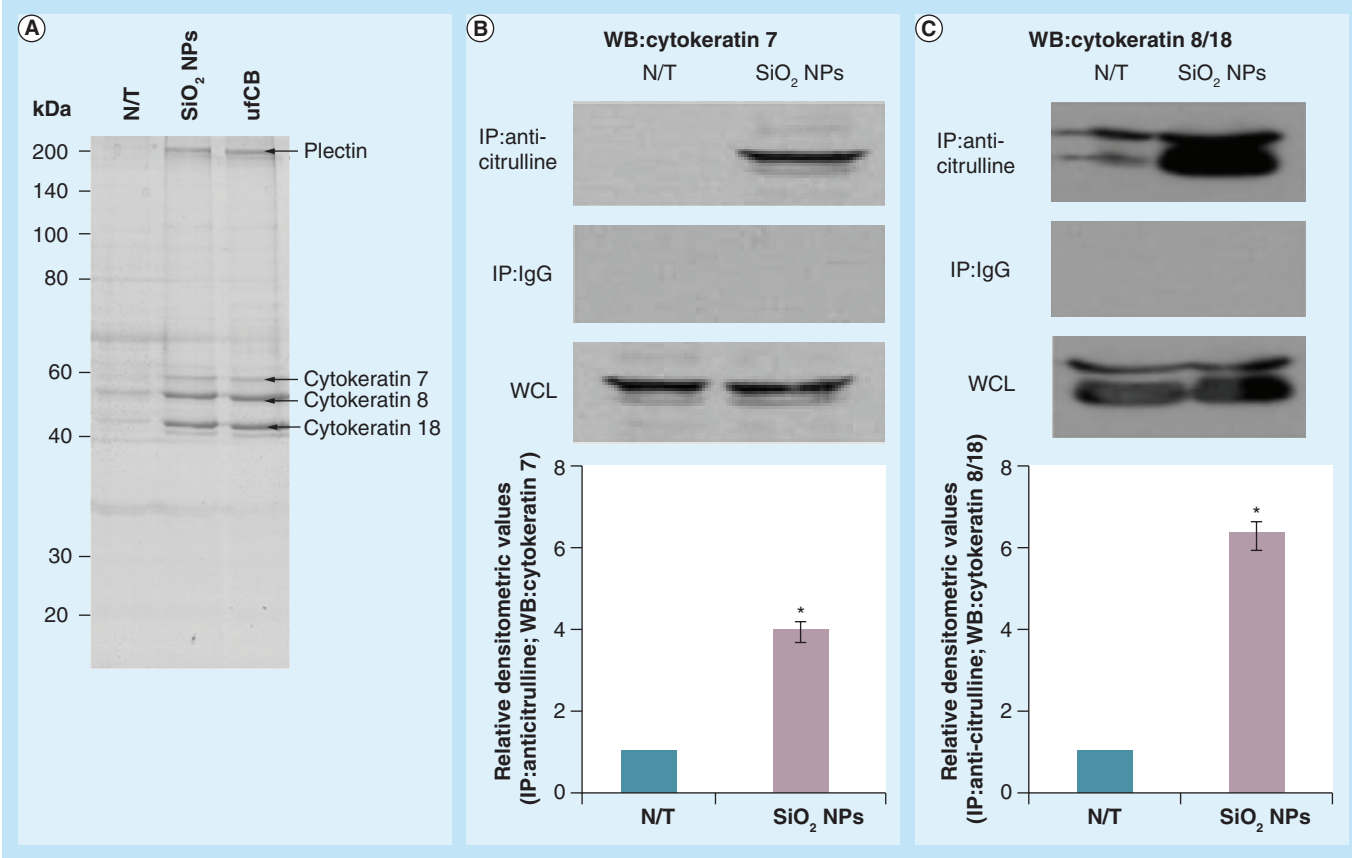

Figure 6. Proteomic analysis of citrullinated proteins. A549 cells (N/T) were exposed to 500 µg/ml 80 nm, SiO_2 NPs or 40 µg/ml ufCB for 24 h and were then lysed. **(A)** Cell lysates (1 mg each) were immunoprecipitated using anticitrulline antibody (Millipore, cat# 07-377), resolved by SDS-PAGE (10% gel) and visualized by colloidal coomassie blue staining. Bands of interest, as indicated, were excised and processed for subsequent mass spectrometric analysis. **(B & C)** Cell lysates (500 µg each) were immunoprecipitated with anticitrulline antibody (immunoprecipitated:anticitrulline) or IgG (isotype control; immunoprecipitated:IgG). Immunoprecipitates and WCLs (used as a control 20 µg each) were WB and probed with **(B)** anticytokeratin 7 or **(C)** anticytokeratin 8/18. Relative densitometric analysis of the individual band was performed and presented. Data are mean ± standard error of mean of three independent experiments.
*Statistically significant data: $p < 0.05$.
NP: Nanoparticle; N/T: No treatment; SiO_2: Silicon dioxide; ufCB: Ultra-fine carbon black; WB: Western blotted; WCL: Whole-cell lysate.

peptides/proteins is that the self-proteins modified by virtue of cell damage and/or uncontrolled apoptosis turn out to be capable of priming autoimmune responses. Our study is the first report demonstrating that NPs of different origin were capable of promoting citrullination of proteins. We have shown that exposure to SiO_2 NPs, ufCB and SWCNTs accelerated accumulation of citrullinated proteins found both in cultured human cells and in the lungs of mice exposed to respirable SWCNTs. Furthermore, we demonstrated that the protein citrullination occurred due to activation of PAD. Several proteins, for example, cytokeratines 7, 8 and 18, and plectins were identified as targets for citrullination, potentially acquiring antigenic properties. These findings provide evidence that NPs could be quite immune-reactive and possibly able to facilitate autoimmune responses. Therefore, keeping in mind the broad application of nanomaterials for drug delivery, implants and medical devices, assessments of their ability to provoke post-translational protein citrullination are warranted. Thus, further investigations are necessary to fully explore the mechanisms of immune outcomes elicited by nanomaterials.

Protein citrullination is one of the post-translational modifications where peptidylarginine residues of the target protein(s) are converted to peptidylcitrulline by PAD enzymes [26–28,53]. Post-translational modifications of proteins influence their structure and biological functions [22]. In fact, some of the post-translationally modified proteins may generate neoepitopes responsible for the pathogenesis of autoimmune diseases including RA. The conversion of arginine to citrulline has been shown to increase peptide–MHC

affinity and activate T cells in transgenic mice [54], ultimately inducing immune responses. In our study, cytokeratins, the largest intermediate filament protein subgroup [55,56] were shown to undergo citrullination after treatment with nanomaterials. Another target of citrullination identified in this study was plectin, which is an important component of the cytoskeleton [57]. Post-translational citrullination of these proteins in response to nanomaterials has not previously been reported. Citrullination of vimentin, fliggrin and histone proteins has been reported in various autoimmune diseases [30,50,53,58].

In recent studies, post-translational protein/amino acid modifications, for example, carbamylation (CM) and/or homocitrullination were linked to inflammation, uremia, atherogenesis and autoimmune diseases including RA [59,60]. CM is the nonenzymatic irreversible reaction of cyanate with amino, hydroxy or thiol groups. *In vivo*, amino group modification resulting in altered function of proteins/amino acids has been observed in patients suffering from uremia due to urea-derived cyanate. These data indicated that CM could impair the free radical and hypochlorous acid scavenging of thiol-amino acids, reducing their protective property against low-density lipoprotein atherogenic modification by oxygen species [61]. Given that exposure to particles trigger an inflammatory response, including markedly increased levels of myeloperoxidase-rich neutrophils, one can assume that CM of protein lysines (with the formation of homocitrulline) can occur in nanosized particle exposed animals. However, in our experiments, neutrophil response found in BAL of mice exposed to respirable SWCNTs occurred on day 7 postexposure (63×10^3 cells/BAL). On day 28 postexposure the amounts of neutrophils declined (17.3×10^3 cells/BAL) [62]. Therefore, the detected marked (2.8-fold) increase of protein citrullination at this late time-point after the exposure was not likely to be dependent on neutrophils accumulation and/or myeloperoxidase activity. We have previously seen that exposure to respirable SWCNTs elicited inflammation, pulmonary damage, modified cytokine pattern in the lung and suppressed systemicimmunity. The mechanism(s) of altered systemic immunity was, to some extent, due to direct effects of SWCNTs on pulmonary dendritic cells [63].

Previously, in epidemiological studies, it was shown that exposure to nanosized SiO_2 NP, droplets of mineral-oil and ufCB increased the risk of RA [3,4,10,11,12]. It has been reported that exposure of mice to diesel exhaust particles (DEPs) augmented both the incidence and the severity of collagen-induced arthritis. DEPs increased production of anti-CII IgG, IgG2a, and IgG1 antibodies, as well as secretion of IFN-γ. These results suggested that Th1 but not Th2 response was triggered by DEPs in collagen-induced arthritis [64,65]. Combustion-derived ufCB, a major air pollutant in urban areas, has been linked to increased incidence of respiratory, cardio-vascular diseases and RA [1,2,6]. Notably, smokers with chronic obstructive pulmonary disease have a relatively high amount of citrullinated proteins [12,66]. Exposure to cigarette smoke was associated with higher expression of the PAD2 enzymes in the lungs [67]. Adjuvant properties of DEPs, ufCB and SWCNTs have previously been reported [64,65,67]. The presence of autoantibodies against citrulline-containing proteins is well documented in RA patients and serves as one of the accepted diagnostic tests [12,13,21–25,53]. Augmented levels of citrullinated proteins may certainly contribute to adjuvant properties of carbonaceous nanomaterials.

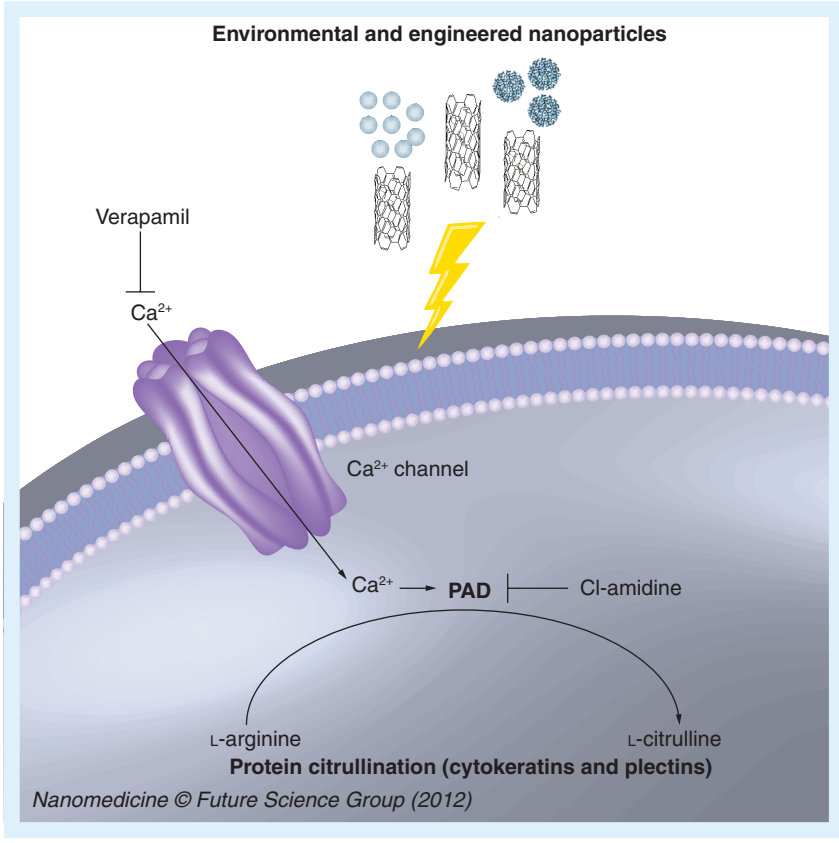

Figure 7. Mechanism(s) of nanomaterials-induced protein citrullination.
Exposure to nanomaterials increases intracellular Ca^{2+}. Elevation of cytosolic Ca^{2+} results in subsequent activation of PADs, which in turn cause citrullination of target proteins (cytokeratins and plectins). Blocking of Ca^{2+} channels or inhibition of PAD activity downregulates protein citrullination.
PAD: Peptidylargininedeiminase.

It is well-established that intracellular Ca^{2+} plays a vital role in PAD activation [26,51,57]. We observed increased intracellular Ca^{2+} in the cells exposed to SiO_2 NPs, SWCNTs and ufCB. Nanomaterials have been shown to accelerate extracellular Ca^{2+} influx via compromised cell membrane integrity [68–70]. Nanosized titanium dioxide has been shown to increase levels of cytosolic Ca^{2+} in human bronchial ChaGo-K1 epithelial cells [68]. To explore if nanomaterials mediated Ca^{2+} influx led to PAD-dependent protein citrullination, human epithelial A549 and phagocytic THP-1 cells were exposed to SWCNTs, ufCB and SiO_2 NPs in the presence of a Ca^{2+}channel blocker. Blocking of the Ca^{2+} channel with verapamil resulted in alleviated protein citrullination. Direct inhibition of PAD by Cl-amidine reduced protein citrullination. However, Cl-amidine and/or verapamil failed to fully inhibit protein citrullination in human THP-1 cells perhaps due to constitutively low PAD4 inherently found in these cells. Proposed mechanism(s) of nanomaterial-induced protein citrullination is outlined in Figure 7. Tissue-specific expression of various isoforms of PAD has been reported [26–28]. In humans, PAD2 is expressed in skeletal muscle, the uterus, brain, salivary glands and pancreas. PAD4 is primarily expressed in macrophages, neutrophils and eosinophils [26–28,52]. PADs are mainly localized in the cytosol of mammalian cells. Citrullination is essential for the formation of neutrophil extracellular traps [30] and site-specific citrullination was reported to alter chemokine function [31–33]. When professional phagocytes were incubated with unmodified hen egg lysozyme, citrullinated peptides were expressed on dendritic cells and peritoneal macrophages facilitating the stimulation of citrulline-specific T-cell responses [71]. Noteworthy, subcellular localization of PADs was found at the sites of inflammation, where citrullinated proteins were elevated [29]. Importantly, both transcriptional and translational regulation govern PAD2 and PAD4 expression in monocytes and macrophages, possibly depending on various stages of their development and cytokine milieu [26,27]. Further studies are required to fully explore intimate mechanism(s) involved in nanomaterial-mediated PAD activation.

Overall, our study demonstrated that nanomaterials of distinct origin, morphology and physicochemical properties were able to induce protein citrullination via increased Ca^{2+}-mediated PAD activity in human cells and animals.

Future perspective

In the years to come, one can expect the increasing variety of nanomaterials to be introduced in everyday life and biomedical applications. Altered immune response developing as a result of human exposure to NPs via the citrullination-dependent mechanism could contribute to the pathogenesis of autoimmune diseases such as RA. Thus, further investigations exploring the nature and mechanisms of immune outcomes elicited by nanomaterials are warranted.

Disclaimer

The findings and conclusions in this report are those of the authors and do not necessarily represent the views of the National Institute for Occupational Safety and Health.

Acknowledgements

BM Mohamed and NK Verma both contributed equally. AA Shvedova and Y Volkov are both senior writers who contributed equally.

Executive summary

Background

- Exposure to silica nanoparticles has been reported to be associated with an increased risk of developing rheumatoid arthritis. Smoking, which has long since been considered a nonspecific risk factor causing chronic inflammation, is now also known to be associated with autoimmune diseases, including rheumatoid arthritis.

Materials & methods

- Several types of nanoparticles of different origin, including silicon dioxide, ultrafine carbon black and single-walled carbon nanotubes were applied to human cells *in vitro* and also investigated in the *in vivo* model of mice exposed to respirable single-walled carbon nanotubes.

Results

- This is the first report demonstrating the induction of protein citrullination in human cells and in mouse lung tissues following exposure to nanosized silica or carbon-derived nanomaterials.
- We have identified and validated the presence of citrulline residues in the cytoskeletal proteins: cytokeratins and plectins.
- Nanomaterial-induced citrullination of proteins was consistent with Ca^{2+}-mediated activation of PAD activity.

Conclusion

- It is proposed that nanomaterials facilitate post-translational citrullination of proteins, which can contribute to the development of autoimmune diseases, including rheumatoid arthritis.

Silica nanoparticles were kindly provided by K Dawson, Centre for BioNano Interactions, University College Dublin, Ireland. We are grateful to VE Kagan, L Tormey, Y Williams and J Conroy for their helpful discussions.

Financial & competing interests disclosure

This work was supported, in part, by the EU FP6 project NanoInteract (NMP4-CT-2006-0333231), SFI SRC Bionanointeract, HEA PRTLI cycles III–IV, NIH grant GM079357, NIOSH NORA/NTRC grant 1927ZHF, EU FP7 project NAMDIATREAM (NMP-2009-LARGE-3–246479) and EU FP7 project NANOMMUNE (EC-FP-7-NANOMMUNE-214281). The authors have no other relevant affiliations or financial involvement with any organization or entity with a financial interest in or financial conflict with the subject matter or materials discussed in the manuscript apart from those disclosed.

No writing assistance was utilized in the production of this manuscript.

Ethical conduct of research

The authors state that they have obtained appropriate institutional review board approval or have followed the principles outlined in the Declaration of Helsinki for all human or animal experimental investigations. In addition, for investigations involving human subjects, informed consent has been obtained from the participants involved.

References

Papers of special note have been highlighted as:
▪▪ of considerable interest

1 André N. Air pollution-related illness: effects of particles. *Science.* 308, 804–806 (2005).

2 Sun Q, Hong X, Wold LE. Cardiovascular effects of ambient particulate air pollution exposure. *Circulation* 121, 2755–2765 (2010).

3 Gilmour PS, Ziesenis A, Morrison ER *et al.* Pulmonary and systemic effects of short-term inhalation exposure to ultrafine carbon black particles. *Toxicol. Appl. Pharmacol.* 195, 35–44 (2004).

4 Williams PR, Phelka AD, Paustenbach DJ. A review of historical exposures to asbestos among skilled craftsmen (1940–2006). *J. Toxicol. Environ. Health B Crit. Rev.* 10, 319–377 (2007).

5 El-Ansary A, Al-Daihan S. On the toxicity of therapeutically used nanoparticles: an overview. *J. Toxicol.* 2009, 754810 (2009).

6 Shvedova AA, Kisin E, Murray AR *et al.* Inhalation vs aspiration of single-walled carbon nanotubes in C57BL/6 mice: inflammation, fibrosis, oxidative stress, and mutagenesis. *Am. J. Physiol. Lung Cell Mol. Physiol.* 295, L552–L565 (2008).

▪▪ **A clear demonstration of the effect of single-walled carbon nanotubes inhalation on induction of inflammatory response, oxidative stress, collagen deposition and fibrosis leading to pulmonary toxicity.**

7 Ryman-Rasmussen JP, Cesta MF, Brody AR *et al.* Inhaled carbon nanotubes reach the subpleural tissue in mice. *Nat. Nanotechnol.* 4, 747–751 (2009).

8 Schwartz J. Harvesting and long term exposure effects in the relation between air pollution and mortality. *Am. J. Epidemiol.* 151, 440–448, (2000).

9 Farhat SC, Silva CA, Orione MA *et al.* Air pollution in autoimmune rheumatic diseases: a review. *Autoimmun. Rev.* 11, 14–21, (2011).

10 Stolt P, Kallberg H, Lundberg I *et al.* Silica exposure is associated with increased risk of developing rheumatoid arthritis: results from the Swedish EIRA study. *Ann. Rheum. Dis.* 64, 582–586 (2005).

▪▪ **This report raised awareness to silica exposure-associated risks in the development of rheumatoid arthritis.**

11 Stolt P, Bengtsson C, Nordmark B *et al.* Quantification of the influence of cigarette smoking on rheumatoid arthritis: results from a population based case–control study, using incident cases. *Ann. Rheum. Dis.* 62, 835–841 (2003).

12 Klareskog L, Stolt P, Lundberg K *et al.* A new model for an etiology of rheumatoid arthritis: smoking may trigger HLA-DR (shared epitope)-restricted immune reactions to autoantigens modified by citrullination. *Arthritis Rheum.* 54, 38–46 (2006).

▪▪ **A breakthrough study linking etiology, a specific genotype and smoking as an environmental hazard with the induction of specific autoimmunity in rheumatoid arthritis patients.**

13 Lukens JR, Dixit VD, Kanneganti TD. Inflammasome activation in obesity-related inflammatory diseases and autoimmunity. *Discov. Med.* 12, 65–74 (2011).

14 Hart JE, Laden F, Puett RC, Costenbader KH, Karlson EW. Exposure to traffic pollution and increased risk of rheumatoid arthritis. *Environ. Health Perspect.* 117, 1065–1069 (2009).

15 Wottrich R, Diabaté S, Krug HF.Biological effects of ultrafine model particles in human macrophages and epithelial cells in mono- and co-culture. *Int. J. Hyg. Environ. Health* 207, 353–361 (2004).

16 Choi SJ, Oh JM, Choy JH. Toxicological effects of inorganic nanoparticles on human lung cancer A549 cells. *J. Inorg.Biochem.* 103, 463–471 (2009).

17 Eom HJ, Choi J. Oxidative stress of silica nanoparticles in human bronchial epithelial cell, Beas-2B. *Toxicol. In Vitro* 23, 1326–1332 (2009).

18 Chen M, von Mikecz A. Formation of nucleoplasmic protein aggregates impairs nuclear function in response to SiO_2 nanoparticles. *Exp. Cell. Res.* 305, 51–62 (2005).

19 Konduru NV, Tyurina YY, Feng W *et al.* Phosphatidylserine targets single-walled carbon nanotubes to professional phagocytes *in vitro* and *in vivo*. *PLoS ONE* 4, e4398 (2009).

20 Kurien BT, Hensley K, Bachmann M, Scofield RH. Oxidatively modified autoantigens in autoimmune diseases. *Free Radic. Biol. Med.* 41, 549–556 (2006).

21 Vossenaar ER, Robinson WH. Citrullination and autoimmune disease: 8th Bertine Koperberg meeting. *Ann. Rheum. Dis.* 64, 1513–1515 (2005).

22 Gyorgy B, Toth E, Tarcsa E, Falus A, Buzas EI. Citrullination: a posttranslational modification in health and disease. *Int. J. Biochem. Cell Biol.* 38, 1662–1677 (2006).

23 Nishimura K, Sugiyama D, Kogata Y *et al.* Meta-analysis: diagnostic accuracy of anti-cyclic citrullinated peptide antibody and rheumatoid factor for rheumatoid arthritis. *Ann. Intern. Med.* 146, 797–808 (2007).

24 Klareskog L, Ronnelid J, Lundberg K, Padyukov L, Alfredsson L. Immunity to citrullinated proteins in rheumatoid arthritis. *Annu. Rev. Immunol.* 26, 651–675 (2008).

25 Lundberg K, Nijenhuis S, Vossenaar ER *et al.* Citrullinated proteins have increased immunogenicity and arthritogenicity and their presence in arthritic joints correlates with disease severity. *Arthritis Res. Ther.* 7, R458–R467 (2005).

26 Vossenaar ER, Radstake TR, van der Heijden A *et al.* Expression and activity of citrullinating peptidylarginine deiminase

enzymes in monocytes and macrophages. *Ann. Rheum. Dis.* 63, 373–381 (2004).

27 Vossenaar ER, Zendman AJ, Van Venrooij WJ, Pruijn GJ. PAD, a growing family of citrullinating enzymes: genes, features and involvement in disease. *Bioessays* 25, 1106–1118 (2003).

28 Foulquier C, Sebbag M, Clavel C *et al.* Peptidyl arginine deiminase type 2 (PAD-2) and PAD-4 but not PAD-1, PAD-3, and PAD-6 are expressed in rheumatoid arthritis synovium in close association with tissue inflammation. *Arthritis Rheum.* 56, 3541–3553 (2007).

29 Willis VC, Gizinski AM, Banda NK *et al.* N-α-benzoyl-N5-(2-chloro-1-iminoethyl)-L-ornithine amide, a protein arginine deiminase inhibitor, reduces the severity of murine collagen-induced arthritis. *J. Immunol.* 186, 4396–4404 (2011).

30 Wang Y, Li M, Stadler S*et al*. Histone hypercitrullination mediates chromatin decondensation and neutrophil extracellular trap formation. *J. Cell Biol.* 184, 205–213 (2009).

31 Struyf S, Noppen S, Loos T *et al*. Citrullination of CXCL12 differentially reduces CXCR4 and CXCR7 binding with loss of inflammatory and anti-HIV-1 activity via CXCR4. *J. Immunol.* 182, 666–674 (2009).

32 Proost P, Loos T, Mortier A *et al.* Citrullination of CXCL8 by peptidylargininedeiminase alters receptor usage, prevents proteolysis, and dampens tissue inflammation. *J. Exp. Med*. 205, 2085–2097 (2008).

33 Loos T, Mortier A, Gouwy M *et al.* Citrullination of CXCL10 and CXCL11 by peptidylargininedeiminase: a naturally occurring posttranslational modification of chemokines and new dimension of immunoregulation. *Blood* 112, 2648–2656 (2008).

34 Barnes CA, Elsaesser A, Arkusz J *et al*. Reproducible comet assay of amorphous silica nanoparticles detects no genotoxicity. *Nano Lett.* 8, 3069–3074 (2008).

35 Shvedova AA, Fabisiak JP, Kisin ER *et al.* Sequential exposure to carbon nanotubes and bacteria enhances pulmonary inflammation and infectivity. *Am. J. Respir. Cell Mol. Biol.* 38, 579–590 (2008).

36 Causey CP, Thompson PR An improved synthesis of haloaceteamidine-based inactivators of protein arginine deiminase 4 (PAD4). *Tetrahedron Lett*. 49, 4383–4385 (2008).

▪ **This work has introduced a solution-phase synthesis of Cl-amidine, which is the most potent of PAD4 inactivators described to date.**

37 Williams Y, Byrne S, Bashir M *et al*. Comparison of three cell fixation methods for high content analysis assays utilizing quantum dots. *J. Microsc.* 232, 91–98 (2008).

38 Mercer RR, Scabilloni J, Wang L *et al.* Alteration of deposition pattern and pulmonary response as a result of improved dispersion of aspirated single-walled carbon nanotubes in a mouse model. *Am. J. Physiol. Lung Cell Mol. Physiol.* 294, L87–L97 (2008).

39 Mohamed BM, Feighery C, Kelly J *et al*. Increased protein expression of matrix metalloproteinases -1, -3, and -9 and TIMP-1 in patients with gluten-sensitive enteropathy. *Dig. Dis. Sci.* 51, 1862–1868 (2006).

40 Pham NA, Morrison A, Schwock J *et al*. Quantitative image analysis of immunohistochemical stains using a CMYK color model. *Diagn. Pathol.* 2, 8 (2007).

41 Verma NK, Dourlat J, Davies AM *et al.* STAT3-stathmin interactions control microtubule dynamics in migrating T-cells. *J. Biol. Chem.* 284, 12349–12362 (2009).

42 Verma NK, Dempsey E, Conroy J *et al.* A new microtubule-targeting compound PBOX-15 inhibits T-cell migration via post-translational modifications of tubulin. *J. Mol. Med.* 86, 457–469 (2008).

43 Verma NK, Dempsey E, Freeley M *et al.* Analysis of dynamic tyrosine phosphoproteome in LFA-1 triggered migrating T-cells. *J. Cell. Physiol.* 226, 1489–1498 (2011).

44 Kozak K, Bakos G, Hoff A *et al*. Workflow-based software environment for large-scale biological experiments. *J. Biomol. Screen.* 15, 892–899 (2010).

45 Freeley M, Bakos G, Davies A, Kelleher D, Long A, Dunican D. A high-content analysis toolbox permits dissection of diverse signaling pathways for T lymphocyte polarization. *J. Biomol. Screen.* 15, 541–555 (2010).

46 Mohamed BM, Verma NK, Prina-Mello A *et al*. Activation of stress-related signalling pathway in human cells upon SiO_2 nanoparticles exposure as an early indicator of cytotoxicity. *J. Nanobiotechnology* 9, 29(2011).

▪▪ **This study demonstrated and described the importance of subtle biological changes downstream of primary membrane and endocytosis-associated phenomena following the high dose of silica nanoparticle exposure.**

47 Birmingham A, Selfors LM, Forster T *et al*. Statistical methods for analysis of high-throughput RNA interference screens. *Nat. Methods* 6, 569–575 (2009).

▪▪ **The publication provides an excellent guidance on the selection of analysis techniques in the context of a sample workflow in high-throughput screening studies.**

48 Knuckley B, Causey CP, Pellechia PJ, Cook PF, Thompson PR. Haloacetamidine-based inactivators of protein arginine deiminase 4 (PAD4): evidence that general acid catalysis promotes efficient inactivation. *Chembiochem.* 11, 161–165 (2010).

49 Knuckley B, Causey CP, Jones JE *et al.* Substrate specificity and kinetic studies of PADs 1, 3, and 4 identify potent and selective inhibitors of protein arginine deiminase 3. *Biochemistry* 49, 4852–4863 (2010).

50 Luo Y, Arita K, Bhatia M *et al.* Inhibitors and inactivators of protein arginine deiminase 4: functional and structural characterization. *Biochemistry* 45, 11727–11736 (2006).

51 Li P, Yao H, Zhang Z *et al.* Regulation of p53 target gene expression by peptidylargininedeiminase 4. *Mol. Cell. Biol.* 28, 4745–4758 (2008).

52 Kearney PL, Bhatia M, Jones NG *et al.* Kinetic characterization of protein arginine deiminase 4: a transcriptional corepressor implicated in the onset and progression of rheumatoid arthritis. *Biochemistry* 44, 10570–10582 (2005).

53 Snir O, Widhe M, Hermansson M *et al.* Antibodies to several citrullinated antigens are enriched in the joints of rheumatoid arthritis patients. *Arthritis Rheum.* 62, 44–52 (2010).

54 Hill JA, Southwood S, Sette A *et al.* The conversion of arginine to citrulline allows for a high-affinity peptide interaction with the rheumatoid arthritis-associated HLA-DRB1*0401 MHC class II molecule. *J. Immunol.* 171, 538–541 (2003).

55 Coulombe PA, Omary MB. 'Hard' and 'soft' principles defining the structure, function and regulation of keratin intermediate filaments. *Curr. Opin. Cell. Biol.* 14, 110–122 (2002).

56 Alix-Panabieres C, Vendrell JP, Slijper M *et al.* Full-length cytokeratin-19 is released by human tumor cells: a potential role in metastatic progression of breast cancer. *Breast Cancer Res.* 11, R39 (2009).

57 Wiche G. Role of plectin in cytoskeleton organization and dynamics. *J. Cell Sci.* 111, 2477–2486 (1998).

58 Asaga H, Yamada M, Senshu T. Selective deimination of vimentin in calcium ionophore-induced apoptosis of mouse peritoneal macrophages. *Biochem. Biophys. Res. Commun.* 243, 641–646 (1998).

59 Wang Z, Nicholls SJ, Rodriguez ER *et al.* Protein carbamylation links inflammation, smoking, uremia and atherogenesis. *Nat. Med.* 13, 1176–1184 (2007).

60 Mydel P, Wang Z, Brisslert M*et al.* Carbamylation-dependent activation of T cells: a novel mechanism in the

pathogenesis of autoimmune arthritis. *J. Immunol.* 184, 6882–6890 (2010).

61 Schreier SM, Steinkellner H, Jirovetz L *et al.* *S*-carbamoylation impairs the oxidant scavenging activity of cysteine: its possible impact on increased LDL modification in uraemia. *Biochimie.* 93, 772–777 (2011).

62 Shvedova AA, Kisin ER, Mercer R *et al.* Unusual inflammatory and fibrogenic pulmonary responses to single walled carbon nanotubes in mice. *Am. J. Physiol. Lung Cell Mol. Physiol.* 289, 698–708 (2005).

63 Tkach AV, Shurin GV, Shurin MR *et al.* Direct effects of carbon nanotubes on dendritic cells induce immune suppression upon pulmonary exposure. *ACS Nano.* 26, 5755–5762 (2011).

64 Yoshino S, Sagai M. Enhancement of collagen-induced arthritis in mice by diesel exhaust particles. *J. Pharmacol. Exp. Ther.* 290, 524–529 (1999).

65 Yoshino S, Hayashi H, Taneda S, Sagai M, Mori Y. Effect of diesel exhaust particle extracts on collagen-induced arthritis in mice. *Autoimmunity* 35, 57–61 (2002).

66 Makrygiannakis D, Hermansson M, Ulfgren AK *et al.* Smoking increases peptidylargininedeiminase 2 enzyme expression in human lungs and increases citrullination in BAL cells. *Ann. Rheum. Dis.* 67, 1488–1492 (2008).

67 Madl AK, Pinkerton KE. Health effects of inhaled engineered and incidental nanoparticles. *Crit. Rev. Toxicol.* 39, 629–658 (2009).

68 Chen EYT, Garnica M, Wang Y-C, Chen C-S, Chin W-C. Mucin secretion induced by titanium dioxide nanoparticles. *PLoS ONE* 6, e16198 (2011).

69 Stone V, Tuinman M, Vamvakopoulos JE *et al.* Increased calcium influx in a monocytic cell line on exposure to ultrafine carbon black. *Eur. Respir. J.* 15, 297–303 (2000).

70 Chen J, Hessler JA, Putchakayala K *et al.* Cationic nanoparticles induce nanoscale disruption in living cell plasma membranes. *J. Phys. Chem. B.* 113, 11179–11185 (2009).

71 Ireland J, Herzog J, Unanue ER. Cutting edge: unique T cells that recognize citrullinated peptides are a feature of protein immunization. *J. Immunol.* 177, 1421–1425 (2006).

Websites

101 Konstanz Information Miner. www.knime.org (Acccessed 12 June 2010)

102 HiTS. http://code.google.com/p/hits,0.3.0 (Acccessed 12 June 2010)

Affiliations

- **Bashir M Mohamed**
Department of Clinical Medicine, Trinity College Dublin, Ireland
- **Navin K Verma**
Department of Clinical Medicine, Trinity College Dublin, Ireland
and
Centre for Research on Adaptive Nanostructures & Nanodevices, Trinity College Dublin, Ireland
- **Anthony M Davies**
Department of Clinical Medicine, Trinity College Dublin, Ireland
- **Aoife McGowan**
Department of Clinical Medicine, Trinity College Dublin, Ireland
- **Kieran C Staunton**
Department of Clinical Medicine, Trinity College Dublin, Ireland
and
Centre for Research on Adaptive Nanostructures & Nanodevices, Trinity College Dublin, Ireland
- **Adriele Prina-Mello**
Department of Clinical Medicine, Trinity College Dublin, Ireland
and
Centre for Research on Adaptive Nanostructures & Nanodevices, Trinity College Dublin, Ireland
- **Dermot Kelleher**
Department of Clinical Medicine, Trinity College Dublin, Ireland
- **Catherine H Botting**
BMS Mass Spectrometry & Proteomics Facility, University of St Andrews, Scotland, UK
- **Corey P Causey**
Department of Chemistry & Biochemistry, University of South Carolina, SC, USA
- **Paul R Thompson**
Department of Chemistry & Biochemistry, University of South Carolina, SC, USA
and
Department of Chemistry, The Scripps Research Institute, FL, USA
- **Ger JM Pruijn**
Department of Biomolecular Chemistry, Radboud University Nijmegen, Nijmegen-Midden, The Netherlands
- **Elena R Kisin**
National Institute for Occupational Safety & Health (NIOSH), WV, USA
- **Alexey V Tkach**
National Institute for Occupational Safety & Health (NIOSH), WV, USA
- **Anna A Shvedova**
National Institute for Occupational Safety & Health (NIOSH), WV, USA
and
Department of Pharmacology & Physiology, West Virginia University, WV, USA
- **Yuri Volkov**
Department of Clinical Medicine, Trinity College Dublin, Ireland
and
Centre for Research on Adaptive Nanostructures & Nanodevices, Trinity College Dublin, Ireland